Creating Enhanced Maps for Lane-Level Vehicle Navigation

David Bétaille, *Member, IEEE*, and Rafael Toledo-Moreo, *Member, IEEE*

***Abstract*—The concept of enhanced maps (Emaps) was introduced with one main objective: It should characterize roads, first, with more completeness and, second, with more accuracy than standard maps to fulfill the requirements of new challenging road safety applications and advanced driver-assistance systems (ADAS). This paper introduces a paradigm for Emap definition and creation on which every road lane is represented and topologically connected to the rest of lanes. Following this approach, a number of Emaps have been created in France, Germany, and Sweden. The experiments carried out in these test sites with the Emaps show the capability of our Emap definition to assist with the determination of the vehicle position at the lane level. Details of the processes of extraction and connection of the road segments are given in the core of this paper, as well as a discussion of the elaboration process and future guidelines in the conclusion.**

***Index Terms*—Enhanced maps (Emaps), Kalman filter, vehicle positioning and navigation.**

I. Introduction

GLOBAL Positioning System (GPS) is the key system in automotive applications, but its limitations are well known in complex environments that cause satellite masking. Other sensors, which are known as inertial navigation sensors (e.g., odometers and gyroscopes), proved necessary in aiding the satellite-positioning process. Literature includes hundreds of references that address the hybridization of inertial measurement units and GPS receivers, in either loose, tight, or even ultratight coupling modes. Some of the most interesting can be found in [1]–[8].

Moreover, except in the improbable case of an absolute desert, the vehicle location itself has no real interest, unless it is related to local georeferenced information. Roads and streets, as well as a couple of other "objects" (in the meaning of database contents), model and structure our environment, and most automotive applications make use of not only vehicle location but digital maps as well. In addition, several authors have shown that map data itself can be of great interest in the so-called map-aided location (MAL) processes [9]–[11], because *a priori* information about the vehicle trajectory is given.

Du *et al.* [12] suggested a classification of automated vehicle location systems into three classes.

1) The first is macroscale, where one finds systems usually set up for car navigation, the accuracy of which has an order of magnitude of 10 m [13]. At this scale, autonomous GPS and usual road database perfectly match.
2) Microscale encompasses every system that builds up local mapping and generally makes use of computer vision, based on camera or lidar images [14]–[16]. Robotics applications typically operate such submeter accurate location systems and, concerning intelligent transportation systems (ITS), advanced driver-assistance systems (ADAS), such as lane-keeping or parking systems. An extensive research effort has been made in road scene analysis, including particular landmarks and road marking recognition, and pedestrian and obstacle detection. Most microscale applications do not require that map objects be referenced with absolute coordinates (i.e., independent of the vehicle body frame), but this could be of great interest in case of cooperative systems, where positioning information is shared between several vehicles and the infrastructure.
3) Last, but not the least, are mesoscale systems, for which vehicle environments are neither regular road sections nor local areas but in-between. This scale concerns multiple-lane crossroads, turn pockets, or off ramps, and many situations where lane-level accuracy is required [12]. Therefore, many applications would benefit from or be enabled by not only better positioning [e.g., with differential GPS (DGPS)] but better maps as well since usual maps become inaccurate and incomplete. With these applications being obviously cooperative, map data should be georeferenced with absolute coordinates.

II. Map Data for Navigation: A State of the Art

Car navigation systems, such as most geographical information systems (GISs), represent roads with one or two polylines (depending on whether lanes with opposite driving directions are physically separated), i.e., a series of nodes and shape points, connected by segments [17]. Nodes have a topological

Manuscript received January 16, 2009; revised August 11, 2009 and March 23, 2010; accepted May 3, 2010. Date of publication July 1, 2010; date of current version December 3, 2010. This work was carried out in the frame of the European project Cooperative Vehicle Infrastructure Systems (CVIS) by researchers with the Geo localization Division, partners of the Positioning and Mapping subproject POMA of CVIS, and the group of Intelligent Systems and Telematics/University of Murcia, which was awarded as an excellence researching group in the frames of the Spanish Plan de Ciencia y Tecnología de la Región de Murcia under Grant 04552/ 1006 GERM/06. The Associate Editor for this paper was D. Srinivasan.

D. Bétaille is with the Laboratoire Central de Ponts et Chaussées, 44341 Bouguenais, France (e-mail: david.betaille@lcpc.fr).

R. Toledo-Moreo is with the Department of Electronics and Computer Technology, Technical University of Cartagena, 30202 Caratagena, Spain, and also with the Intelligent Systems and Telematics Group, University of Murcia, 30003 Murcia, Spain (e-mail: rafael.toledo@upct.es).

Color versions of one or more of the figures in this paper are available online at http://ieeexplore.ieee.org.

Digital Object Identifier 10.1109/TITS.2010.2050689

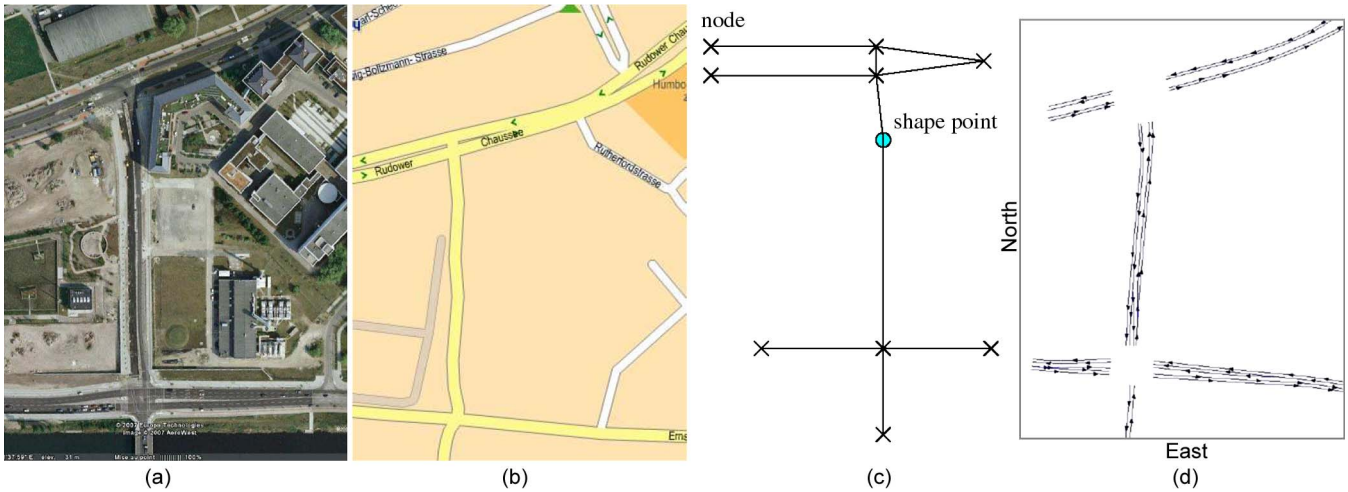

Fig. 1. (a) Google Maps image of the test site in Berlin (Germany) where an Emap was developed. (b) Visualization of a standard map of the area. (c) Representation of this area with segments and node and shape points. (d) Emap of the same area.

interest, because they stand for either crossroads or junctions (entrances or exits), whereas shape points provide a spatial sampling of the road to which they belong (see Fig. 1).

Moreover, what is modeled has limited accuracy from global and local points of view.

1) Globally: Many digital maps often show similar inaccuracy as paper versions: Maps are neither always exactly scaled nor coherent from one "page" to another. Similar techniques (photogrammetry) are used for traditional and digital cartography, leading to similar drawbacks. The accuracy level of standard maps today is about 5 m (for metropolitan areas) up to 20 m.
2) Locally: Road geometry is approximated by a series of shape points, with a level of approximation that meets the macroscale requirements of navigation systems today. Between shape points, a linear interpolation appears feasible with no need for any polynomial of higher degree, which simplifies positioning projection and map rendering. Therefore, the actual distance between a chord (i.e., a segment defined by two consecutive shape points) and the ground truth arc may exceed 1 m in curves and even more dramatically in roundabouts, where one can find a simple node representation. A higher spatial sampling would obviously contribute to locally improve the modeling of road geometry. Nonetheless, a compromise is introduced between the error of the interpolation process on the one hand and the capacity of the data storage and its real-time access on the other hand.

However, ADAS concerned by mesoscale positioning systems, such as flexible lane allocation, that are enhanced by not only driver awareness but also lane keeping or autocruise control at microscale cannot solely rely on the standard GIS representation due to its inaccuracy and its incompleteness. To sum up, global and local errors, as well as missing contents, would not only cause at least mismap-matching but also make it impossible for applications at lane-level accuracy.

These applications were judged to be relatively feasible within a decade by the authors of the well-known Enhanced Digital MAPping (EDMAP) project final report for the U.S. Department of Transport (DoT) and Federal Highway Administration [18]. This report highlights that, while satellite positioning has made significant progress with various DGPS networks (local or global, and private or public), as well as satellite augmentations in North America, Japan, and Europe, map quality remains one step behind in most commercial services that are available off the shelf today.

New developments seem to be under progress in most map provider R&D teams [19], [20] to bridge the gap still existing between mapping standards and ADAS requirements. The idea would be to keep standard polyline representation, in accordance to geographic data files, and add the necessary geometrical attributes for ADAS, such as the typical number of lanes and even lane widths. Every cross section could be detailed that way in terms of geometry (with, between consecutive cross sections, linear interpolation) and added to standard road maps, as an additional attribute of road segments. Experiments (e.g., in SafeSpot IP [21]) that will help to draw conclusions about the fulfillment of the ADAS requirements are ongoing.

Other map data become available at large scale, e.g., in France, Institut Géographique National provides a first data collection that contains a 3-D city model, including 2-D areas for pedestrian, cycles, cars, and buses within the new frame called référentiel à grande échelle (RGE). Ongoing research projects (such as CityVIP [22]) should make these new data "navigable" in terms of real-time access by a map engine.

III. Emap Model Proposition

The enhanced map (Emap) model that we suggest in this paper further goes in terms of both accuracy and contents. To provide applications with a comprehensive description of the road, each carriage way and each lane are described (see Fig. 1), which figures out a set of "nominal" middle-lane trajectories on the modeled road. Note that crossroads have been removed from the scope of this geometrical representation since they allow too many trajectories possible.

Instead of spatially sampling with shape points, we suggest an alternative that consists of using standards regarding road geometry, i.e., (for plane design) a series of straight lines,

circles, and clothoids (spiral curve). They all obey the same curvilinear 2-D equations, with null, constant, and linearly variable curves, respectively. In a Cartesian frame, these equations are functions of the curvilinear abscissa, i.e., the distance performed along the curve. These functions are not explicit, but they are given under the form of the following Fresnel's integrals:

$$x(l) = x_0 + \int \left(\cos(\tau_0 + \kappa_0 l + \frac{cl^2}{2} \right) dl, \qquad 0 < l < L$$
$$y(l) = y_0 + \int \left(\sin(\tau_0 + \kappa_0 l + \frac{cl^2}{2} \right) dl, \qquad 0 < l < L$$

where

x_0, y_0 initial coordinates of the curve;
τ_0 initial bearing of the curve;
κ_0 initial curvature;
c curvature rate with the curvilinear abscissa $(d\kappa/dl)$, with $\kappa = \kappa_0 + cl$;
l curvilinear abscissa;
L total length of the curve.

In the last years, clothoids have been applied for curvature tracking in some ADAS applications [23]. In our work paper, we suggest its exploitation for the description of the road lanes stored in a digital map. The definition of road elements of an Emap by means of clothoids presents some benefits, compared with the most common polyline-based method. Indeed, clothoids fit the actual road shape better, which decreases the amount of information to be stored in the database.

The map construction process, based on mobile mapping and designed for test purposes in our laboratory, is detailed later on.

IV. Mobile Mapping and Determination of Emap Geometry

Mobile mapping is already a way of directly collecting road network geometry by circulating the area to map. Most map providers collect and process information with dedicated vehicles that are equipped with calibrated sensors, with the aim of positioning and mapping all surrounding roads, lane marking, and signs and deploying automatic object recognition. Coupling kinematic GPS in postprocessing (PPK) and dead reckoning (DR) has the main advantage of continuously delivering the final result almost directly with no bias.

Similarly as [24] and [25], one may expect a series of the aforementioned curves hidden in mobile mapping data. The next algorithm consists of extracting analytical equations that best fit the performed trajectories. We systematically repeat mobile mapping and determination of the geometry for all lanes of the Emap, regardless of their usual parallelism. This way, singular change in road cross section or lane width will cause no trouble. The key point is to survey each lane, driving as close as possible to its center and as far as possible when it merges with another.

On a complex interchange area or in a city center, a comprehensive mobile mapping necessarily induces a certain redundancy in the data collection: some sections will be circulated twice or more, which requires manual cut at data processing. In addition, any eventual specific maneuvers made during the data collection have to be suppressed before their use for mapping. Depending on whether a visual inspection of the itinerary is possible offline (monitoring the images of a front camera vision for instance), the operator must not forget to log event markers whenever obstacles have to be avoided, leading to a nonnominal trajectory.

Note that another interesting way of collecting data was investigated by U.S. project EDMAP in the beginning of the 2000th, based on the fusion of the trajectories given by a fleet of GPS equipped cars [26], [27]. This approach is known under the name "probe data."

A. Extraction Process

Let us remark here that the vehicle trajectory is *a priori* computed at the decimeter accuracy level with PPK and DR. Smoothing (such as backward process) during this computation in postprocessing is also recommended. The determination of straight lines and circles among a sequence of surveyed points is efficiently solved with least squares: Newton–Raphson or Levenberg–Marquadt's methods can be applied in this context. However, we aim at fitting geometrical elements closer than 5 cm to the vehicle trajectory, which could lead to a large number of lines and circles. Moreover, geometrical transitions between the identified elements still remain difficult to achieve since linking the extremities of consecutive straight lines and circles makes sudden discontinuities if no long-enough clothoids are fitted between. As a consequence, we have given priority to these transitions in the extraction process, and since clothoids have the advantage of the generic form (which degenerates into circles or lines zeroing one or two parameters), we will propose a clothoids-only extraction process.

Let us assume that the longitudinal geometry of a lane is a stochastic process, variable as a function of the performed distance along this lane, with *a priori* unknown parameters x_0, y_0, τ_0, κ_0, and c. This set of parameters encompasses either straight lines, circles, or actually clothoids. With respect to this process, GPS (or GPS + DR) locations can be considered as observations. The dynamics of this process can be deduced from the Fresnel's integrals, with a second-order Taylor's development, which copes with their nonexplicit expression

$$x(l + dl) = x(l) + \cos(t)dl - \frac{\kappa \sin(t) dl^2}{2}$$
$$y(l + dl) = y(l) + \sin(t)dl + \frac{\kappa \cos(t) dl^2}{2}$$

with

$$t = t_0 + \kappa_0 l + \frac{cl^2}{2} \quad \text{and} \quad \kappa = \kappa_0 + cl.$$

and dl denotes the elementary distance performed to compute the integrals. In the following, dl is considered as an input in the prediction process. We fixed its value at 1 cm.

This process fits the state-space and Markovian chain representation suitable for Kalman filtering, with a vector composed of the main variable l plus the parameters to identify x_0, y_0, t_0, κ_0, and c, plus x and y resulting from the integration.

For simplification and robustness purposes, x_0 and y_0 have not been included in the identification process, and their value will be fixed by the first GPS + DR observation.

Thus, in discrete representation, the prediction model is

$$\begin{aligned} l(k+1|k) &= l(k|k) + dl \\ \tau_0(k+1|k) &= \tau_0(k|k) \\ \kappa_0(k+1|k) &= \kappa_0(k|k) \\ c(k+1|k) &= c(k|k) \\ x(k+1|k) &= x(k|k) + \cos(t)dl - \frac{\kappa \sin(t) dl^2}{2} \\ y(k+1|k) &= y(k|k) + \sin(t)dl + \frac{\kappa \cos(t) dl^2}{2} \end{aligned}$$

with

$$\begin{aligned} \tau &= \tau_0(k|k) + \kappa_0(k|k) l(k|k) + \frac{c(k|k) l(k|k)^2}{2} \\ \kappa &= \kappa_0(k|k) + c(k|k) l(k|k) \end{aligned}$$

and the observation model is

$$\begin{aligned} x_{\mathrm{GPS+DR}} &= x(k+1|k) \\ y_{\mathrm{GPS+DR}} &= y(k+1|k). \end{aligned}$$

In matrix notation, this gives

$$X = [l \quad t_0 \quad \kappa_0 \quad c \quad x \quad y]' \tag{1}$$

and P denotes its variance–covariance matrix.

The prediction and observation models in matrix notation are

$$\begin{aligned} X(k+1|k) &= f\left(X(k|k), U(k+1) + \nu_U\right) + \nu_{\mathrm{Mod}} \\ U(k+1) &= dl \\ Y_{\mathrm{GPS+DR}} &= \begin{bmatrix} 0 & 0 & 0 & 0 & 1 & 0 \\ 0 & 0 & 0 & 0 & 0 & 1 \end{bmatrix} X(k+1|k) + \nu_{\mathrm{GPS+DR}} \end{aligned}$$

where ν_U, ν_{Mod}, and $\nu_{\mathrm{GPS+DR}}$ represent the prediction, input, and observation noise vectors, respectively. Both input and observation noise vectors are assumed to be normally distributed with means equal to zero. They are therefore characterized by their variance.

1) Input variance, e.g., $Q = dl^2$ in m^2. With dl equal to 1 cm, the integration error between GPS points typically separated by a few meters will consequently have an order of magnitude of the decimeter (i.e., the square root of a few hundreds of elementary centimeter dl errors integrated). This progress of the error is comparable to the possible observation error below (fixed kinematic GPS), which enables outlier detection. Therefore, a local decimeter plane accuracy is guaranteed. Thus, related to the traveled distance (for usual clothoids, which are generally a few tens of meters and sometimes more than 100 m), the global accuracy of the extended Kalman filter (EKF) estimated parameters is always lower than 10^{-2} rad for the initial heading, 10^{-3} m^{-1} for the initial curvature, and 10^{-4} m^{-2} for the curvature rate. (These parameters are linked together by the inverse of the curvilinear abscissa, which at least cumulates until 10 m.) This is shown in Fig. 4.

2) Observation variance, e.g.,

$$R = \begin{bmatrix} 0 & 0.2^2 \\ 0.2^2 & 0 \end{bmatrix}$$

in square meter in areas where fixed kinematic GPS solutions are available. Note that R should vary along with the *a posteriori* statistics of the GPS + DR fusion output. Let us remark here that, since fixed kinematic solutions are employed, GPS position values were always accurate enough in terms of direction. Therefore, there is no need to employ GPS velocity values.

The prediction error will be considered as negligible with respect to the integrated input error. Thus, the prediction noise vector will be set to zero.

With f being a nonlinear function, its Jacobian matrices Jf_X and Jf_U with respect to X and U will be computed and used to update P, i.e.,

$$P(k+1|k) = Jf_X P(k|k) Jf_X' + Jf_U Q Jf_U'.$$

The EKF formulation gives the *a posteriori* variance–covariance matrix

$$\begin{aligned} P(k+1|k+1) = (I - P(k+1|k) \\ \times H' \left(HP(k+1|k)^{-1} H' + R\right) H) P(k+1|k). \end{aligned}$$

After a few iterations, this state-space system should converge onto a correct estimation of the geometrical parameters. The theory stands that a minimum of four observation points are required for a clothoid, similar to three or two for a circle or a straight line, respectively.

What this method cannot perform is the determination of several clothoids in the same process. In practice, clothoids have to be extracted one after the other, which makes necessary regular resets of the filtering process. The conditions for stop and start clothoids have to be discussed now.

B. Conditions for Detecting Clothoid Transitions

In statistical terms, a transition should correspond to the violation of the hypothesis along which all consecutive points would belong to the same clothoid.

The statistical test on the normalized innovation squared (NIS, which is also called Mahalanobis distance, where the innovation is the distance between the predicted point $[x(k+1|k), y(k+1|k)]'$ and the observed $Y_{\mathrm{GPS+DR}}$ solutions) that one applies to any new observation is necessary, but not sufficient is this extraction problem. This test is applicable to any new point since it can be considered as doubtful with regard to the current clothoid, i.e.,

$$\begin{aligned} \mathrm{NIS} = (Y_{\mathrm{GPS+DR}} - HX(k+1|k))' \\ \cdot (HP(k+1|k)H' + R)^{-1} (Y_{\mathrm{GPS+DR}} - HX(k+1|k)). \end{aligned}$$

In a χ^2 test, this distance should be compared to a threshold that depends on, first, the degree of freedom of the system and, second, the probability of nondetection that one accepts for this test. When a GPS + DR observation makes NIS exceed the χ^2

threshold, then a probable outlier has been detected. However, in case this point is accepted, it is not presumable whether the new clothoid that includes this point should remain coherent with the previous observations. It therefore appears that a more complete test is required.

Thus, after every estimation step, the new clothoid (which includes the very last accepted GPS + DR point) is checked as given here.

1) If previous GPS + DR points are found to lie further than 5 cm to this clothoid, this means that it has been shifted away by the current GPS + DR point.
2) A counter is incremented whenever the preceding test concludes to an invalidation and decremented otherwise.
3) When this counter exceeds 4, one considers that a new clothoid has started.

Four is the minimum number of points needed to fit a clothoid.

Then, a new clothoid has started. This entails a reset of the parameters contained in the state vector (and a registration of the latest validated parameters).

The map construction is founded on heuristic rules that we shall briefly discuss now. The most critical one concerns the distance threshold employed to decide whether the positioning points are close enough to the current clothoid line, or a new clothoid must begin. In our experiments, this value is set to 5 cm. This tolerance is actually compliant with trajectories obtained in postprocessing, with kinematic GPS solutions (those using phase double differences between the rover and a local base station) fused with inertial integration (odometer plus gyroscope) and smoothed, e.g., in a Rough backward filter [28]. In this fusion process, the characterization of the GPS positioning error plays the major role: 5 cm corresponds to the expected accuracy of ambiguity fixed PPK GPS. We have tried to introduce DGPS solutions, instead of PPK. Even those with meter accuracy that can be obtained under good Wide Area Augmentation System (WAAS)/European Geostationary Navigation Overlay Service (EGNOS) conditions do not comply with the 5-cm threshold. If this tolerance is unchanged, many DGPS solutions (even fused with inertial navigation) are considered as outliers, and almost no clothoids are found, except when a series of points are (by chance) harmoniously organized along a certain curve. Of course, 5 cm can be raised up to 25 cm for instance, which makes many more clothoids extracted but with rather short length and short radius of curvature: The resulting geometry using WAAS/EGNOS GPS is unacceptable.

V. Experimental Validation

The sensors placed on board the mobile mapper were the following:

1) Zmax kinematic GPS receiver logging at 10 Hz;
2) KVH RD2100 fiber-optic single-axis gyroscope used at 10 Hz;
3) encoder mounted on the gearbox of the rear-wheel Ford van, with a step of 0.2615 m.

The same GPS receiver was set up in the vicinity of the test site: the maximum length of the baseline between both receivers did not exceed 5 km.

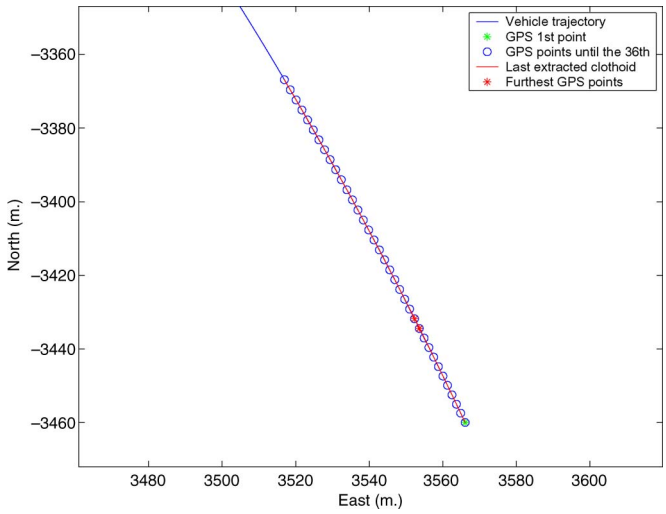

Fig. 2. Extracted clothoid (solid red) using the first 36 points. When introducing the 36th point of the GPS + DR vehicle trajectory (solid blue), there appears two previous points that deviate from the clothoid by more than 5 cm.

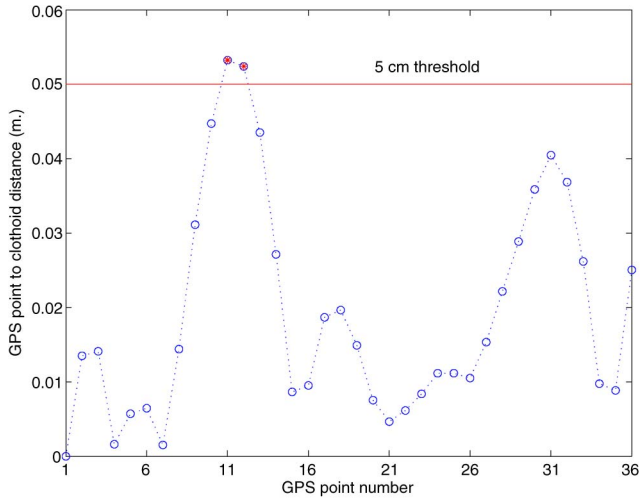

Fig. 3. Residual distance between the last extracted clothoid and the first 36 GPS + DR points used for its extraction. The 5-cm threshold is exceeded by two points, which indicates that a new clothoid should start just after the 36th GPS + DR point.

GPS data were postprocessed with Global Navigation Satellite Systems (GNSS) solutions. The obtained navigation solutions were fused in an optimal Raugh smoother with the gyro and odometer data [28].

Figs. 2 and 3 show, on the extraction of the first element, the invalidation of the observation update corresponding to the 36th GPS + DR point. When this point is introduced, it appears that the previous 11th and 12th locations are further than 5 cm from the current clothoid, although they passed through the NIS test before (which makes sense because they are actually not outliers). Fig. 4 shows the predicted standard deviations of the six state vector components of (1) until the 36th GPS + DR observation. Fig. 5 shows the series of clothoids extracted from a GPS + DR trajectory of our mobile mapper in a loop of the Cheviré Bridge south interchange.

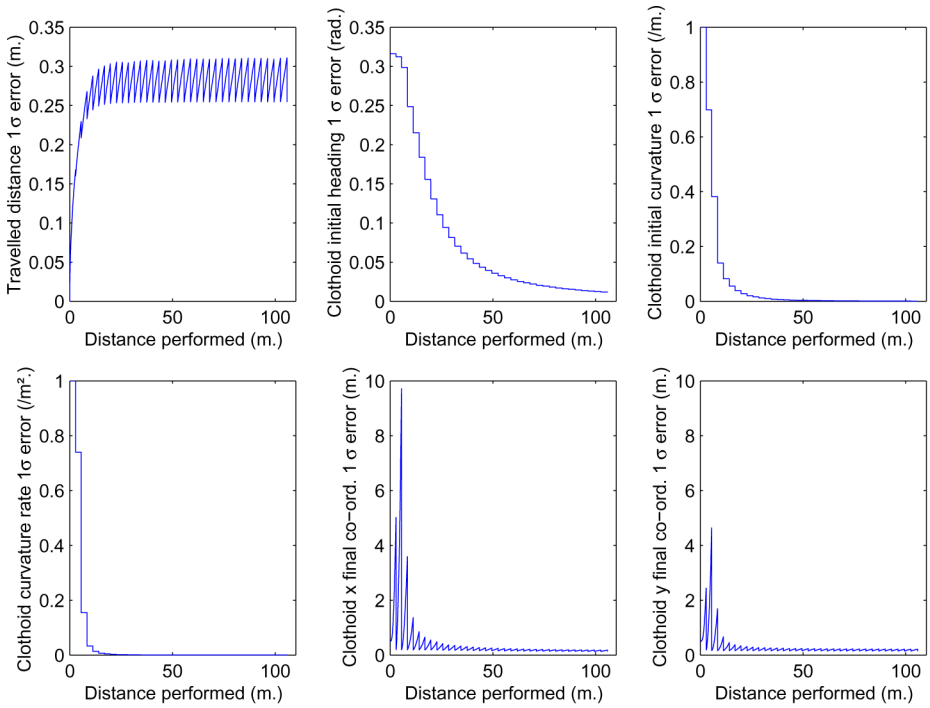

Fig. 4. Standard deviations output by the EKF. They apply to the six components of the state-space vector. In the prediction/estimation process, standard deviations increase at prediction and decrease at estimation, which explains the pattern in the figures. The clothoid parameters progressively converge, whereas additional GPS + DR points are included.

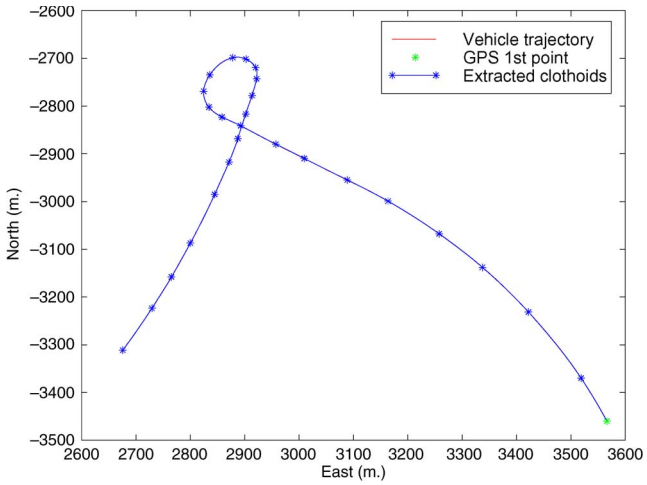

Fig. 5. Extract of the final Emap. (One lane only is shown here.) (Solid red) The vehicle trajectory is hidden by (solid blue) the series of clothoids at the scale of this figure.

VI. Connectivity of Lane Segments

The aimed Emap not only consists of a set of segments that describe the geometry of the road but also includes topological information of these segments. Contrary to standard maps where the topology of the map is associated to the nodes, in our proposal, the segments are linked to their neighbors. This way, the Emap considerations assume that a vehicle may realize a transition from a segment to another at any point of the first. The transitions are therefore not artificially bounded to the segment nodes, giving more flexibility to the positioning system.

In an earlier state of our investigations, the connectivity links among the road segments previously extracted were manually established. Despite the fact that this intensive and tedious task can be done offline, the convenience of an automated procedure to associate road segments seems quite clear to save time and possible errors in the process of manual labeling. Next in this section, it will be proven that, attending the geometrical aspects of the segments and traffic considerations, it is possible to automatically establish the connectivity relations among the segments of an Emap like that proposed in this paper. This section presents the process of finding the road segments to which it is possible to make a transition from a known one. An earlier development of this method can be found in [29]. In this new version, more detailed topological aspects that allow easier navigation based on the Emap are included. The new functionalities that the Emap includes in its current version are given as follows:

1) characterization of left, right, and front neighbors;
2) relative lateral position of the lane segment at every road stretch;
3) improved method for the determination of the connectivity between two segments;
4) more efficient computational approach that is capable of establishing the complex connectivity map in a shorter time.

The rest of this section is organized as follows: First, the strategy followed regarding traffic regulations is discussed. In the next sections, the concepts of neighbor segments, candidate segments, and common nodes are introduced. Next, the different algorithms applied to determine the nature of the connectivity among the Emap segments are presented. After that, the process of establishing the relative lateral position of

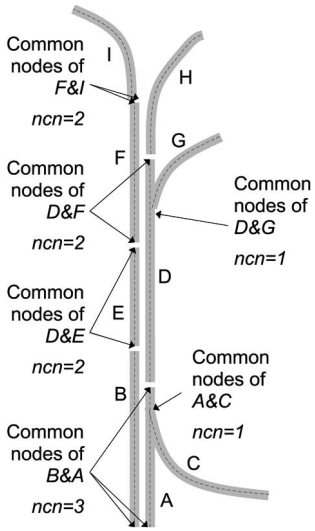

Fig. 6. Scheme representation of road segments with different cases under study on a highway. (Black dashed line) Center line of the lane segment. (Gray) Area of the lane segment. The driving direction is from south to north. A common node between two segments is any extremity of these segments that is very close to any point of the other segment. On the upper side of the image, there is an example of the driving direction criterion: (Bottom to top) The connection $F2I = 1$, whereas $I2F = 0$. (A displacement from I to F is not accepted.) Different examples of common nodes between pairs of segments are presented, representing situations of $ncn = 1, 2,$ and 3.

each segment of the Emap is explained. Finally, some further remarks including computational aspects are discussed.

A. Traffic Regulation Policy

We decided against including all traffic rules and regulations in the process since, in many cases, it is actually feasible for a vehicle to perform a maneuver that is not allowed in that particular place. This brings more flexibility to meet real traffic situations or temporary changes in the signalization of the road. On the other hand, the total rejection of traffic regulations in the process of linking segments unnecessarily increases the computation of the positioning algorithm since, de facto, many assumed linked segments will not be used in most usual cases [17]. Following the recommendations for future map-matching algorithms made by Quddus *et al.* [17], a compromise between both strategies was finally decided: Road directions and those cases with strict regulations, such as remarkable median-strip solid lines or forbidden directions in road stretches with single or multiple lanes, were contemplated.

B. Definition of Neighbor Segments and Emap Fields

Our task entails finding those road segments in which the vehicle could be when it will leave the current road segment. After that, we must characterize these connected segments as front, left, or right neighbors. That way, the connectivity concept defined in our approach is not bijective and will have a concrete direction. Therefore, it can be found feasible to make a transition from segment F to segment I, which is noted as $F2I = 1$, but not from I to F $(I2F = 0)$. This orientation feature suits well to the traffic restrictions of single direction lanes. Fig. 6 shows an example of this case.

TABLE I
ROAD SEGMENT FORMAT WITHOUT CONNECTIVITY FIELDS

x_0	y_0	z_0	x_L	y_L	z_L	τ_0	κ_0	c_0	L

TABLE II
FIELDS WITH TOPOLOGICAL DESCRIPTION

NLL	RLP	NN	N1	N2	...	T1	T2	...

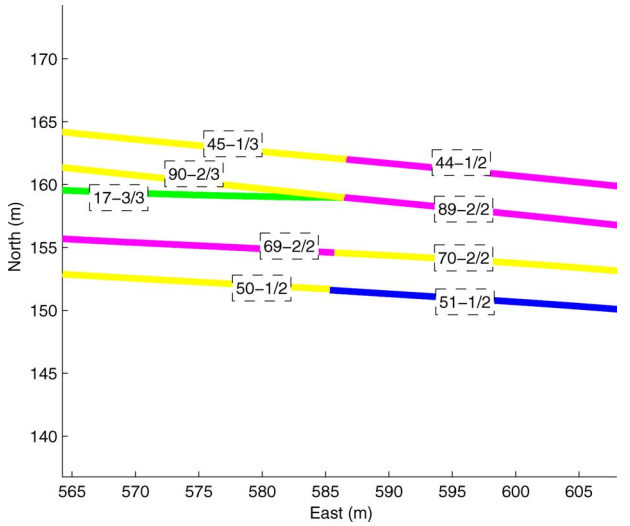

Fig. 7. Example of topological description that includes the relative lateral position in the Emap of Berlin DLR. The fields of the label [44–1/2] indicate [Segment identifier-relative lateral position of the lane (starting from the right)/number of lateral lanes]. At the points where the road topology changes (in the image, segment 17 appears), a new set of clothoids that represent the new topology must begin for the whole cross section.

The description of every individual segment follows the format given in Table I, where four conditions hold.

1) x_0, y_0, and z_0 are the XYZ coordinates of the initial point of the clothoid.
2) x_L, y_L, and z_L are the correspondent for the last point.
3) τ_0, κ_0, and c_0 stand for the initial yaw angle, initial curvature, and its linear rate, respectively.
4) L is the length of the clothoid segment.

Table II presents the topological information that complements the description shown in Table I.

1) NLL and RLP describe the relative lateral position of the segment. NLL stands for the number of lateral lanes in this area, whereas RLP indicates the relative lateral position of the lane within the rest (see Fig. 7). We accept the convention that the first lane of a carriageway with multiple lanes is the one most to the right. For instance, $[\mathtt{NLL} = 3, \mathtt{RLP} = 1]$ indicates that the segment under consideration is the right lane of a carriageway of three lanes. This approach allows supplying the relative position on the road to the user, which can be found very useful in many safety and ADAS applications. On the other hand, individual road segments are forced to start and finish at the points where the topology of the road changes (i.e., one lane appears or disappears), which was formally taken into account in the extraction process.
2) NN represents the number of neighbors linked to this segment.

3) N1, N2, . . ., are the segment identifiers of the neighbors, whereas T1, T2, . . ., indicate if the connection with segment NX is front (TX = 1), left (TX = 2), or right (TX = 3). Although NN could easily be calculated from the number of NX fields different from −1 (which represents an empty field), it has been found useful to include its value in the Emap to speed up the computations needed at the moment of collecting the segment information by a positioning algorithm. In addition, no noticeable augmentation of the Emap file size was found due to this field (typical values vary between 0 and 7).

Next step will be filling up the fields of identifiers for every road segment of the Emap. Since bijective relations between segments were disregarded, it is assumed that the application of the results obtained from one segment in the study of another does not bring any particular benefit to our algorithm. On the contrary, taking into consideration bijective relations diminishes the capability to automatically find connected segments as it makes every case much more specific, this being our main reason to neglect that option. Consequently, we follow the simplest strategy of finding connected segments for only one road segment at one step, which implies the systematical repetition of the algorithm as many times as segments are in the map.

C. Preselection of Candidates

Let us assume that the vehicle is, at the present time, in the road segment A. Our first task is to preselect possible candidates that verify that a transition from A to them would be feasible. To realize this, we decided to start by following a simple strategy of looking for those segments with any point closer to a certain distance to any point of segment A. The computation of this may be high, but since, at this moment of the algorithm, there is no need for very accurate values of distance, the whole process can quickly be accomplished. By taking into account the frequency of most common GPS/DR navigation systems (usually higher than 5 Hz), and vehicle and road speed limitations, a resolution value of 1 m and a distance criterion of 5 m were selected (and they were found suitable). As a result of the preselection process, in the trials performed, it was found that all segment connections were detected, with the final number of connected segments being typically half of the number of candidates.

One consideration related to altitude values along segments must be done. Since the positioning algorithm developed in our investigations assumes a local tangent plane, there is no need to employ the altitude of the road for data fusion. However, this becomes necessary to discriminate those segments that cross the road at upper or lower altitudes and therefore are not "in contact" with the current segment, which appears to be very frequent in highways and urban rings.

According to the way roads are actually built, vertical alignments follow straight and parabolic definitions [24]. Taking into account that the average values of segment lengths in our Emaps are between 50 and 70 m, it can be found that the approximation of all the vertical alignments to straight line definitions is sufficiently precise for our purposes, whereas it significantly reduces the computational complexity of the search.

The process of preselecting candidates is therefore affected as follows: When a segment B contains a point B_p that is found within the assumed limits of the neighborhood of a point A_p of segment A, the altitudes of both A_p and B_p are estimated. To do that, we can apply a simple linear equation by using the altitude values in the extremities of both segments, which were stored in the previous phase in the segment data row. When the difference of altitude between points A_p and B_p is higher than a certain threshold, the connection of these two segments is not accepted at these points. In the case that another set of two points of segments A and B was found to be a candidate, the same process is repeated. Typical difference values for crossing roads at different altitude levels were found to be higher than 4 m. Following this value and also taking into account, first, the accuracy of altitude values for the segment extremities and, second, the errors made in the assumption of a linear representation of the segment profile, we tuned the threshold difference to 1.5 m. Nevertheless, because the distance between crossing roads is under normal conditions long enough, the algorithm was not very sensitive to this threshold. Following this simple strategy, no connections were missed in the Emaps developed in our experiments.

D. Concept of Common Nodes

The concept of common node of an Emap segment was first introduced by Bétaille *et al.* [29]. Once again, we hereby include its definition for an easier understanding of the whole process.

Let us assume that a vehicle is in road segment A, and points A_i and A_l define the initial and last extremities of this segment, respectively. Let us also assume that, in the previous phase, we found one candidate segment B, with extremities B_i and B_l. To ease the process of determining if segment B can be a future segment when moving from segment A, we must find the common nodes between these two segments.

In the most common definition of a map, nodes are the extremities of the road segments, and their descriptions include different properties that depend, for example, on whether this segment is connected to some others at this node. In our case, in the analysis of the relation $A2B$, a common node is an initial or last point of A or B that is close (closer than a certain threshold) to any point of the other segment. When an extremity is found to be a common node, its flag is set to 1, with the default state for the relation $A2B$ being $A_i = A_l = B_i = B_l = 0$. For our experiments, the threshold of proximity was established in 5 m. A higher value for this threshold may lead to a higher number of possible common nodes, increasing the posterior computations, whereas a much lower value may cause the loss of real common nodes and is therefore not recommendable. In any case, according to our experiments, the algorithm is not very sensitive to this value: the trials made with values of 4 or 6 m led to the exact same final Emaps.

Fig. 6 shows the concept of common nodes with some examples, where ncn stands for the number of common nodes found between two segments. According to this definition, the process of finding common nodes among the segments linked as candidates is a simple calculation of the distance between their

extremities and the other segment. To do so, the resolution between two consecutive points of one segment was set to 0.1 m.

The next section will explain the algorithms based on the concept of common nodes that were developed to determine whether a candidate segment will be accepted as a neighbor. Let us clarify here our definition of neighbor segment: A segment B is a neighbor of A if the vehicle can directly move from A to B. Thus, the neighbors of A are not all the segments around it.

E. Cases of Study

There are five possible situations in the study of $A2B$, depending on the number of common nodes between A and B, i.e., $ncn_{A2B} : \{0, 1, 2, 3, 4\}$. For every specific case, a custom algorithm is launched to determine the nature of the connection (front, right, or left).

For a clearer understanding, this section is only dedicated to the algorithms capable of determining the relation $A2B = 0, 1$, where 0 means that candidate B is not a neighbor of A and 1 means that it is. After this, we will focus on the type of connectivity.

1) Case $ncn_{A2B} = 0$: This would be the case of a pair of segments that have two points closer than 5 m, but none of their extremities is close to any point of the other segment. This case represents a very unusual situation if we consider that the horizontal alignment of road segments is described by clothoids, and it was never found in our experiments. Nevertheless, one unusual situation that could lead to this case would appear when both clothoids representing segments A and B present high values of curvature, and they are arranged in opposite directions following a scheme such as) (. For this case and to avoid any unexpected result from the algorithm, we decided to include this situation in the code, establishing a positive relation of $A2B = 1$.

2) Case $ncn_{A2B} = 1$: Several situations that match this value are shown in Fig. 6, among which are segments A, C, and D, G. As it can been seen in this figure, this case typically corresponds with lanes that join or leave a carriageway. In the Emap of Berlin, with 93 segments, the case $ncn_{A2B} = 1$ appears ten times. The algorithm applied to determine the connection from A to B, depending on the flag values, is given next.

```
if (A_l = 1) OR (B_i = 1)
  then ⇒ A2B = 1;
else ⇒ A2B = 0;
end
```

The cases corresponding to these conditions can be seen in Fig. 6. When studying $C2A$, it can be seen that $ncn_{C2A} = 1$ and $C_l = 1$, which gives the first case of the OR operator. The second case could be represented by $D2G$, where $G_i = 1$. However, the relations in the opposite directions $A2C$ and $G2D$ are equal to zero since it is not in fact not possible to make these transitions.

3) Case $ncn_{A2B} = 2$: This case represents, by far, the most common situations on a multiple lane road, being, for this reason, the more complex. Some of its possible combinations are represented in Fig. 6. The algorithm is organized, depending on the common-node flags, as explained next for the case of $A2B$.

```
a) ____________________
   if (B_i = 1) AND (B_l = 1)
     then ⇒ A2B = 1;
b) ____________________
   elseif (A_l = 1) AND (B_l = 1)
     if (dist(A_l, B_l) < 5)
       then ⇒ A2B = 0;
     else ⇒ A2B = 1;
     end
c) ____________________
   elseif (A_l = 1) AND (B_i = 1)
   then ⇒ A2B = 1;
d) ____________________
   elseif (A_i = 1) AND (A_l = 1)
     then ⇒ A2B = 1;
e) ____________________
   elseif (A_i = 1) AND (B_i = 1)
     if (dist(A_i, B_i) < 5)
     then ⇒ A2B = 0;
       else ⇒ A2B = 1;
     end
f) ____________________
   elseif (A_i = 1) AND (B_l = 1)
     if (dist(A_i, B_l) < 5)
       then ⇒ A2B = 0;
     else ⇒ A2B = 1;
     end
____________________
end
```

where $dist(A_x, B_y)$ stands for the Euclidean distance between these two points. Let us analyze now the topologies related to these subcases.

1) Both common nodes belong to the same segment (E2D in Fig. 6).
2) Two segments with opposite directions that go parallel during a stretch. If this stretch is very small (shorter than 5 m), it is assumed that segments are not connected. On the contrary, if the distance is longer, both segments share a stretch where a vehicle could pass from one to another.
3) This is the case of two consecutive segments with the same direction being B ahead, and also the case of two parallel segments with the same direction that share a stretch. Both make $A2B = 1$.
4) This is similar to case 1.
5) This is similar to case 2.
6) This case embraces two options: 1) two consecutive segments when A is the one ahead (and, therefore, $A2B = 0$) and two parallel segments that share one stretch that could allow a lane change.

The case of $ncn_{A2B} = 2$ appears 298 times in the Emap of Berlin DLR (93 segments).

4) Case $ncn_{A2B} = 3$*:* In this case, three of the four possible nodes of A and B are close to at least one point of the other segment, which corresponds to the case of parallel segments than start or finish at very close points (segments A and B in Fig. 6). For this case, it will be accepted that $A2B = 1$ without further considerations. $ncn_{A2B} = 3$ was found 96 times in the Emap of Berlin DLR.

5) Case $ncn_{A2B} = 4$*:* In this last case, all the extremities of both nodes are close to any point of the other. This represents the situation of parallel segments that start and finish at very close points, resulting to $A2B = 1$. This appeared only four times in the Emap of Berlin DLR.

F. Connectivity type

Once it is established whether a transition from segment A to segment B is accepted as feasible, i.e., $A2B = 1$, we proceed to find the nature of this connection. The notation followed goes like this.

1) $A2B = F$, when B is found a front neighbor. (In Fig. 6, I is the front neighbor of F, which is noted by $F2I = F$.)
2) $A2B = L$, when B is found a left neighbor. (In Fig. 6, E is the left neighbor of D, which is represented by $D2E = L$.)
3) $A2B = R$, when B is found a right neighbor. (In Fig. 6, D is a right neighbor of E, which is noted by $E2D = R$.)

Finally, the notation $A2B = 1$ is kept for the cases when the algorithm could not achieve any conclusion about the nature of the relation, but it is still certain that it is possible to travel from segment A to B.

For our reasoning, we will follow a similar strategy based on the same cases and subcases presented in the previous section.

1) Case $ncn_{A2B} = 0$*:* For its peculiarity, we decided to warn that two segments are connected with unknown type.

2) Case $ncn_{A2B} = 1$*:* All the cases of $A2B = 1$ consider that B is a front neighbor of A $(A2B = F)$.

3) Case $ncn_{A2B} = 2$*:* The complexity of this case requires a specific reasoning. It can be established that $A2B = F$ in subcase c when B is after A. In the other subcases where $A2B = 1$, B will be a left or a right neighbor. This decision can be made by applying an algorithm that employs as inputs the geometrical information of the segments under consideration. As a matter of fact, right or left depends on the values of the orientations of the segment A at its common nodes (if any), the orientations of the segment B at the corresponding closer points to the common nodes of A (if any), and the orientations of the vectors from the common nodes (of A and/or B) to their closer points of the neighbor segment. Fig. 8 shows one example of the scheme for the study of $A2B$ in which six conditions hold.

1) Common node 1 belongs to segment A.
2) Common node 2 belongs to segment B.
3) The angle of segment A at common node 1, i.e., τ_1, belongs to the first quadrant.

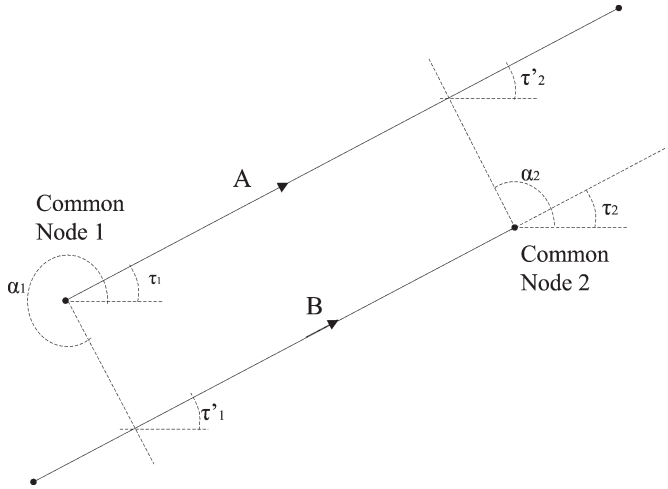

Fig. 8. Example of a scheme of the angles considered in the determination of the lateral type of topology (right–left).

4) The angle of segment B at the point where the normal projection of common node 1 reaches segment B, i.e., τ_1', belongs to the first quadrant.
5) The angle of segment B at common node 2, i.e., τ_2, belongs to the first quadrant.
6) The angle of segment A at the point where the normal projection of common node 2 reaches segment A, i.e., τ_2', belongs to the first quadrant.

Under these conditions, it can be found that

```
if (α1 < τ1) OR (α1 > τ1 + 180°)
  then ⇒ A2B1 = R;
end
```

```
if (α2 > τ2) AND (α2 < τ2 + 180°)
then ⇒ A2B2 = R;
  end
```

```
if (A2B1 = R) AND (A2B2 = R)
  then ⇒ A2B = R;
end
```

Analogous reasonings can be done for the different cases of segment attitudes. Let us remark here that, if the outputs obtained in the analysis done in both common nodes are not coherent, the algorithm maintains the link $A2B = 1$ and launches a warning.

4) Cases $ncn_{A2B} = 3$ *or 4:* These two cases imply a lateral relation between A and B that is finally established analogously as the case $ncn_{A2B} = 2$.

G. Relative Lateral Lane Position

Our Emap includes the information of the relative lateral position of every lane, as referred to its lateral neighbors. An example of this can be seen in Fig. 7. A simple example of the usefulness of this information could be the case when a vehicle drives in a carriageway of three lanes through the lane more

to the left, and the aimed exit (only accessible from the lane more on the right) is approaching. The application must warn the driver that two lane changes should be done to reach the aimed segment.

The algorithm explained next assumes that the maximum number of lanes in a carriageway is four, which is the maximum value found in our test sites. Nevertheless, it is possible to extend it to any number of lanes when required.

Once again, let us assume that the vehicle is in segment A. Let us also define two counters for the number of lanes (NLL) and for the relative lateral position of the vehicle in these lanes (RLP), which are both set by default to 1.

The first step consists of looking for right neighbors of A. If a right neighbor is found (B), both NLL and RLP are increased by one. Next, it is checked whether B has its own right neighbors. In case that there are right neighbors, both counters are again increased by one point. The same strategy is followed until there are no more right neighbors or NLL reaches its maximum value (four in our case).

In the next step, left neighbors are searched. If there are no left neighbors, the values of NLL and RLP are definite. In the case that a left neighbor is found (C), only NLL is increased by one. At this point, we must consider whether C goes in the same direction of segment A. If C goes in the same direction, we must continue looking for left neighbors to determine the final value of NLL. However, if it goes in the opposite direction, we must look for the right neighbors of C, which will actually be lanes situated on the left side of A. The determination of the orientation of C, compared with A, is carried out by simply checking whether C has A as a left (opposite direction) or right (same direction) neighbor.

Let us remark that the case of neighbors with opposite directions when we are looking for right neighbors is not feasible in most countries, except the British Islands, Japan, etc.

H. Further Remarks

The algorithm was designed in such a way that, in case that some incoherent conclusion was found, a warning is given to the user of the software. In the case of the Emap of Cheviré Bridge, 591 segments and 1745 links among segments were found. There appeared 35 cases of $ncn = 1$, with no errors (misassignments) or undefined cases. (A warning is launched to inform that the link could not be automatically defined.) $ncn = 2$ was found in 2214 situations, with seven undefined situations and only one error. $ncn = 3$ appeared 258 times, with only two undefined assignments and no errors. $ncn = 4$ was found 26 times, with only one undefined assignment. Similar values were obtained for every Emap, proving the success of the proposed algorithm.

Regarding the size of the Emaps, that of Cheviré Bridge describes approximately an area of 4 km North and 2 km East with 591 segments in only 88 kB. Berlin DLR describes 600 m North and 700 m East with 93 segments in 12 kB.

Computational considerations were also taken into account to avoid excessive time in the preparation of the connectivity map. Nevertheless, all processes can be executed *a priori* and offline, and therefore, no sharp restrictions in terms of computational time were established. For the case of the Emap of Cheviré Bridge, the process requires less than 2 h in a dual-core laptop at 1.67 GHz running in Matlab and using only one central processing unit for this process.

TABLE III
HPEs IN METERS IN TWO TEST SCENARIOS WITH (S1E, S2E) AND WITHOUT (S1, S2) EMAP UPDATE

Test	Mean	Std	Max.
S1	0.580	0.795	4.049
S1E	0.389	0.405	2.317
S2	4.849	6.635	20.048
S2E	0.279	0.426	2.944

TABLE IV
LANE-ASSIGNMENT RESULTS

Test Scenario	Mismatch percentage	Mismatch time	GNSS blockage duration
S1E	1.8 %	10.9 s	141 s
S2E	1.9 %	4.4 s	45 s

Along this and previous sections, novel algorithms for road segment extraction and connection have been described. It has been shown how, following a semi-automatic manner, it is possible to develop an Emap that is capable of describing the road with accuracy and completeness enough to serve well-advanced applications at the lane level. These algorithms were applied to create prototypes of Emaps in France, Germany, and Sweden. The next section shows the good results in terms of vehicle positioning obtained in field tests where these Emaps were used as observations in an MAL process.

VII. NAVIGATION RESULTS

Although the scope of this paper is not the navigation problem itself but only the creation process of the Emap, some brief results of position accuracy and map matching obtained using our Emap as an input of a navigation and map-matching system are presented now to emphasize the interest of the Emap model in an MAL process. Details of the navigation and map-matching algorithm can be found in [11].

Table III shows the results of the horizontal positioning errors (HPEs) in a set of tests for validation of the Emap and the navigation algorithm itself. The notation S1E indicates that the Emap was used as an input observation during the localization loop in scenario 1, whereas S1 shows that the Emap was not employed (analogous for scenario 2). As it can be seen, the differences between using and not using Emap are noticeable, particularly in scenario 2. In both cases, simulated GNSS masks reproduced bad satellite visibility conditions. The use of the Emap in the localization process can be found to be very beneficial to avoid position drifts from the road path.

Some results regarding map matching obtained in the same two test scenarios are presented now in Table IV. Let us remark that these results also correspond to lane assignment and not only to road assignment. In all the scenarios tested in our experiments, the percentage of correct matches to the road is 100%. Regarding lane assignment, the worst case of all tests appears in test S2E with 1.9% of lane mismatches, which corresponds to 4.4 s. These mismatches occurred after long GNSS absences. The last column of Table IV shows the total

duration of GNSS gaps for every test. In the best case (not shown in the table), 100% of lane assignments were actually correct.

VIII. Conclusions and Future Works

The two main contributions of this work can be summed up as follows.

1) A novel paradigm for the description of the road stored in a digital map that exploits the definition of clothoids to follow the road shape. This approach presents some benefits in terms of accuracy and adaptability to the road shape when compared with the standard maps based on a series of straight lines.
2) A detailed description of the process of building an Emap that is more accurate and complete than standard maps and that meets the requirements of advanced applications aiming the lane level. An EKF is applied to process the vehicle trajectory given by smoothed GPS positions and DR measurements.

Some other aspects and conclusions of interest are discussed next.

1) The construction of the Emap is founded to some extent on heuristic rules. Some of these values may need to be different in some other scenarios. The values presented here have proven to work well in three different scenarios, and the sensitivity of the algorithms was not high. (We found no need for fine tuning.) Nevertheless, it is advisable to supervise the performance of the automatic algorithms and possibly to update these parameters when required. The most desirable way to tune these parameters would be in an automatic fashion based on a numeric description of the scenario under consideration. However, to the authors' mind, this seems to be very difficult since too many different aspects not only of the road geometry but also of the mobile mapping process must be taken into account, such as the frequency of the positioning system, the speed of the test vehicle, and the ability of the driver to remain in the middle lane.
2) The quality of the data obtained by mobile mapping is an important factor that depends on the quality of the positioning sensors and the expertise put in the post-process. We recommend a minimum set of Kinematic GPS hybridized with DR (odometry plus gyroscope). If the scenario to be mapped presents very poor GNSS visibility conditions, the position may need to be enhanced with high-grade inertial navigation. Additionally, it is advisable to employ tightly coupled filters for GNSS/DR fusion if possible since the results are normally better than those obtained by more simple loosely coupled approaches. Techniques for multipath removal are also strongly encouraged since even small multipath may lead to the creation of fake road segments. Although the algorithm for clothoid extraction is robust to noise in GPS + DR positions to a certain extent, the use of noisy positions would yield to an unacceptable description of the road geometry, even if the algorithm would not fail.
3) The majority of complex road scenarios have been considered and modeled so far. However, roundabouts and crossroads were extracted off the map construction process, because, in real traffic conditions, the trajectories of vehicles normally do not follow predefined shapes. For this reason, these concrete scenarios deserve special attention.
4) The successful exploitation of the Emaps and the Emap-aided location will eventually be determined by the final application. It is reasonable to think of scenarios where standard digital maps are complemented by Emaps only in the areas where standard maps cannot provide enough accuracy and completeness to the intended application. The relevance of the application or applications that would benefit from the Emap may or may not justify the investment of building an Emap in an area.

The resulting Emaps were satisfactorily applied to a combined fusion/map-matching algorithm that meets the requirements of ITS applications for positioning and mapping at lane-level accuracy. This algorithm was applied to Emaps in France, Germany, and Sweden, presenting very good results.

For the moment, we have targeted the proof of concept of an Emap that is capable of providing MAL at the lane level. However, similarly as their authors conclude in the DoT report concerning EDMAP, the process designed in the context of this research still has to progress to achieve performance level of industrial production. We believe that a significant reduction in the effort made for producing the first experimental Emaps is really possible in the near future. Among some others, the use of the probe data coming from a large amount of GPS receivers installed in vehicles that frequently drive the same trajectories is of special interest. This approach has the benefit of automatically eliminating errors introduced in the collected data due to special maneuvers and possible driving bias with respect to the middle lane. Another interesting approach is the use of aerial images and visual tools to obtain the mapping points. We have investigated this possibility of obtaining interesting results. These last two approaches deserve much further study and consequently lie out of the scope of this paper.

In this open field of research, we foresee that further progress might still be needed, in terms of map data collection, map construction, and map tracking.

Acknowledgment

The authors would like to thank M. Schingelhof and his team at the German Aerospace Center (DLR), Institute of Transportation Systems, for their work on the data collection in Berlin.

References

[1] J. Farrell and M. Barth, *The Global Positioning System and Inertial Navigation: Theory and Practice*. New York: McGraw-Hill, 1998.
[2] R. M. Rogers, *Applied Mathematics in Integrated Navigation Systems*. Washington, DC: AIAA, 2003, ser. AIAA Education.
[3] R. Toledo-Moreo, M. Zamora, B. Ubeda, and A. F. Skarmeta, "High-integrity IMM-EKF-based road vehicle navigation with low-cost GPS/SBAS/INS," *IEEE Trans. Intell. Transp. Syst.*, vol. 8, no. 3, pp. 491–511, Sep. 2007.

[4] D. Bevly, J. Ryu, and J. Gerdes, "Integrating INS sensors with GPS measurements for continuous estimation of vehicle sideslip, roll, and tire cornering stiffness," *IEEE Trans. Intell. Transp. Syst.*, vol. 7, no. 4, pp. 483–493, Dec. 2006.
[5] Y. Yang and J. Farrell, "Magnetometer and differential carrier phase GPS-aided INS for advanced vehicle control," *IEEE Trans. Robot. Autom.*, vol. 19, no. 2, pp. 269–282, Apr. 2003.
[6] D. Obradovic, H. Lenz, and M. Schupfner, "Fusion of sensor data in Siemens car navigation system," *IEEE Trans. Veh. Technol.*, vol. 56, no. 1, pp. 43–50, Jan. 2007.
[7] S. Sukkarieh, E. Nebot, and H. Durrant-Whyte, "A high integrity IMU/GPS navigation loop for autonomous land vehicle applications," *IEEE Trans. Robot. Autom.*, vol. 15, no. 3, pp. 572–578, Jun. 1999.
[8] S. Cho and W. Choi, "Robust positioning technique in low-cost DR/GPS for land navigation," *IEEE Trans. Veh. Technol.*, vol. 55, no. 4, pp. 1132–1142, Aug. 2006.
[9] Y. Cui and S. S. Ge, "Autonomous vehicle positioning with GPS in urban canyon environments," *IEEE Trans. Robot. Autom.*, vol. 19, no. 1, pp. 15–25, Feb. 2003.
[10] C. Fouque, P. Bonnifait, and D. Bétaille, "Enhancement of global vehicle localization using navigable road maps and dead-reckoning," in *Proc. IEEE ION Position, Location Navig. Syst. Conf.*, Monterey, CA, 2008, pp. 1286–1291.
[11] R. Toledo-Moreo, D. Bétaille, F. Peyret, and J. Laneurit, "Fusing GNSS, dead-reckoning and enhanced maps for road vehicle lane-level navigation," *IEEE J. Sel. Topics Signal Process.*, vol. 3, no. 5, pp. 798–809, Oct. 2009.
[12] J. Du, J. Masters, and M. Barth, "Lane-level positioning for in-vehicle navigation and automated vehicle location (AVL) systems," in *Proc. IEEE Intell. Transp. Syst. Conf.*, Washington, DC, 2004, pp. 35–40.
[13] Portable Satellite Navigation Systems on the Road to Success, 2008. [Online]. Available: www.gfk.com/group/press_information/press_releases/002095/index.en.html
[14] S. Vacek, S. Bergmann, U. Mohr, and R. Dillmann, "Fusing image features and navigation system data for augmenting guiding information displays," in *Proc. IEEE Multisensor Fusion Integr. Conf.*, Heidelberg, Germany, 2006, pp. 323–328.
[15] J. Melo, A. Naftel, A. Bernardino, and J. Santos-Victor, "Detection and classification of highway lanes using vehicle motion trajectories," in *Proc. IEEE ITS Conf.*, Toronto, ON, Canada, 2006, pp. 188–200.
[16] M. Jabbour and P. Bonnifait, "Backing up GPS in urban areas using a scanning laser," in *Proc. IEEE ION PLANS Conf.*, Monterey, CA, 2008, pp. 505–510.
[17] M. A. Quddus, W. Y. Ochieng, and R. B. Noland, "Current map-matching algorithms for transport applications: State-of-the-art and future research directions," *Transp. Res. Part C*, vol. 15, no. 5, pp. 312–328, Oct. 2007.
[18] J. Du *et al.*, CAMP enhanced digital mapping project—Final report, U.S. Dept. Transp., Washington, DC. [Online]. Available: http://www.nhtsa.gov/DOT/NHTSA/NRD/Multimedia/PDFs/Crash%20Avoidance/2004/FinalRept_111904.pdf
[19] C. Zott, S. Y. Yuen, C. L. Brown, C. Bertels, Z. Papp, and B. Netten, "Safespot local dynamic maps: Context-dependent view generation of a platform's state and environment," presented at the 15th Intell. Transp. Syst. World Congr., New York, Nov. 2008, Paper 20260.
[20] K. Wevers and S. Dreher, "Digital maps for lane level positioning," presented at the 15th Intell. Transp. Syst. World Congr., New York, Nov. 2008, Paper 20487.
[21] SafeSpot European Project, Cooperative Vehicles and Road Infrastructure for Road Safety. [Online]. Available: http://www.safespot-eu.org
[22] CityVIP French Project, p. 8, 2007. [Online]. Available: http://www.agence-nationale-recherche.fr/documents/aap/2007/finances/PREDIT-TSFA-resumes-2007.pdf
[23] A. Eidehall, "Tracking and threat assessment for automative collision avoidance," Ph.D. dissertation, Linköping Stud. Sci. Technol., Linköping, Sweden, 2007.
[24] K. Baass and J. Vouland, "Détermination de L'Alignement Routier à Partir de Traces GPS," in *Proc. Congrès Annuel de L'ATC (Association des Transports du Canada)*, Calgary, AB, Canada, 2005.
[25] A. Eidehall, J. Pohl, and F. Gustafsson, "Joint road geometry estimation and vehicle tracking," in *Proc. IEEE Intell. Vehicles Symp.*, 2004, pp. 619–624.
[26] J. Wang, S. Shroedl, K. Mezger, R. Ortloff, A. Joos, and T. Passegger, "Lane keeping based on location technology," *IEEE Trans. Intell. Transp. Syst.*, vol. 6, no. 3, pp. 351–356, Sep. 2005.
[27] S. Shroedl, S. Rogers, and C. Wilson, "Map refinement from GPS traces," DaimlerChrysler Res. Technol. Center North America, Palo Alto, CA, RTC Rep. No. 2000/6, 2000.
[28] D. Bétaille, "GYROLIS: Post-processing of vehicle localization software via GPS-gyrometer-odometer coupling," *Bull. des Laboratoires des Ponts et Chaussées*, no. 272, pp. 75–87, 2008.
[29] D. Bétaille, R. Toledo-Moreo, and J. Laneurit, "Making an enhanced map for lane location based services," in *Proc. IEEE Intell. Transp. Syst. Conf.*, Beijing, China, Oct. 2008, pp. 711–716.

David Bétaille (M'10) received the Ph.D. degree from University College London, London, U.K., in 2004, for his investigations on phase multipath in kinematic Global Positioning Systems.

He is currently a Researcher with the Geolocalization Research Team, Laboratoire Central des Ponts et Chausées, Bouguenais, France, where his current activities relate to vehicle positioning by satellite systems combined with dead reckoning and mapping. Advanced driver-assistance systems and, in general, road-safety applications compose the research context of his laboratory.

Rafael Toledo-Moreo (M'08) received the M.S. degree in automation and electronics engineering from the Technical University of Cartagena (UPCT), Cartagena, Spain, in 2002 and the Ph.D. degree in computer science from the University of Murcia (UMU), Murcia, Spain, in 2006.

He is currently an Associate Professor with the Department of Electronics and Computer Technology, UPCT. He is also a Research Member with the Intelligent Systems and Telematics Group, UMU.

Dr. Toledo-Moreo is a member of the International Federation of Automatic Control Technical Committee on Transportation Systems and the IEEE Robotics and Automation Society Technical Committee for Intelligent Transportation Systems. He is an Associate Editor and member of International Program Committees of several conferences related to intelligent transportation systems and a Guest Editor for one journal.